

# Automatic bilateral filtering of digital X-ray rocking curves using histograms\*

Serhiy Balovsyak<sup>1,†</sup>, Ihor Fodchuk<sup>1,†</sup>, Zhengbing Hu<sup>2,†</sup>, Inna Iakovlieva<sup>1,†</sup>,  
Serhii Yakovliev<sup>1,\*,†</sup>

<sup>1</sup> Yuriy Fedkovych Chernivtsi National University, Kotsiubynsky 2, 58012, Chernivtsi, Ukraine

<sup>2</sup> School of Computer Science, Hubei University of Technology, Wuhan, China

## Abstract

The relevance of the bilateral filtering algorithm for digital signal processing, namely, X-ray rocking curves, has been substantiated. The software for removing noise on digital X-ray curves with automatic determination of the bilateral filter parameters has been developed. The digital bilateral filter has been constructed as a combination of two Gaussian filters that perform signal processing in the intensity domain and in the angular domain. A mathematical model has been developed for calculating the noise level on the curve and the standard deviations of the bilateral filter in the intensity domain and in the angular domain, respectively. The high-frequency component of the signal has been extracted by a Laplace filter. The histogram of the high-frequency component has been calculated, and the acceptable interval for noise values on the high-frequency component has been established. The noise level based on the high-frequency component has been calculated taking into account the established acceptable interval. The software for automatic bilateral filtering of X-ray curves has been developed in the Python. The parameters of bilateral filtering have been set taking into account the results of processing 20 experimental X-ray curves of the train dataset. The bilateral filtering of 10 experimental X-ray curves of the test dataset has been performed. It has been shown that the bilateral filtering of X-ray curves allows not only to significantly reduce their noise level, but also to preserve the shape of the useful signal.

## Keywords

X-ray rocking curves, digital signal processing, noise level, bilateral filtering algorithm, digital filter, histogram, software, Python

## 1. Introduction

Experimental X-ray rocking curves are widely used to study the structure of various materials, in particular crystal ones [1]. X-ray curves are one-dimensional signals, the intensity of which depends on the angle of rotation of the studied sample or the X-ray detector. Analysis of the angular distribution of such curves allows us to obtain information about the structural perfection of the studied samples. However, the analysis of X-ray curves is complicated by the presence of significant noise levels in them, which is especially noticeable in areas of low intensity. Noise distorts the signal shape, which leads to a decrease in the accuracy of determining the parameters of the studied samples. Reducing the noise of X-ray curves and increasing their signal-to-noise ratio at the hardware level is difficult since there are limitations on the power of the primary X-ray beam. In addition, it is technically extremely difficult to reduce the level of noise that occurs in X-ray detectors. Even modern X-ray detectors generate a signal with a certain level of noise [2]. Therefore, the current task is to programmatically reduce the noise level on X-ray curves using digital filtering

---

*Intelitsis'25: The 6th International Workshop on Intelligent Information Technologies & Systems of Information Security, April 04, 2025, Khmelnytskyi, Ukraine*

\* Corresponding author.

† These authors contributed equally.

✉ s.balovsyak@chnu.edu.ua (S. Balovsyak); i.fodchuk@chnu.edu.ua (I. Fodchuk); drzbhu@gmail.com (Zh. Hu); i.yakovlieva@chnu.edu.ua (I. Iakovlieva); yakovliev.serhii@chnu.edu.ua (S. Yakovliev)

ORCID 0000-0002-3253-9006 (S. Balovsyak); 0000-0001-6772-6920 (I. Fodchuk); 0000-0002-6140-3351 (Zh. Hu); 0000-0002-8917-8686 (I. Iakovlieva); 0009-0005-2752-8467 (S. Yakovliev)



© 2025 Copyright for this paper by its authors. Use permitted under Creative Commons License Attribution 4.0 International (CC BY 4.0).

methods [3]. However, in the practical implementation of such signal filtering, distortions occur. For example, common methods of Gaussian [3], median [5] and wavelet [6] filtering lead to blurring of the peaks of the curves. Smoothing of the shape of X-ray curves is observed both during filtering in the spatial domain and during filtering in the frequency domain using the Fourier transforms [7-9]. Compared to Gaussian filtering, wavelet filters lead to less smoothing of peaks, but there is a need to choose the wavelet family and order, method of correcting the wavelet coefficients [10, 11].

According to the criterion of preserving the waveform, one of the most effective is the bilateral filtering algorithm, which processes the signal simultaneously in the spatial (angular) domain and in the intensity domain [12-14]. By taking into account the difference in intensity for different points of the curve, the bilateral filtering algorithm allows to significantly remove noise with minor distortions of the useful signal. However, a certain complexity of the application of bilateral filtering lies in the selection of filter parameters in the spatial domain and in the intensity domain. The selection of such parameters in manual mode is subjective and time-consuming. Therefore, in this work it has been proposed to determine the parameters of the bilateral filter automatically taking into account the noise level on the X-ray curve. To determine the noise level, the high-frequency component of the signal is calculated by the Laplace filter, and the histogram of the obtained high-frequency component is analyzed. Automatic bilateral filtering allows processing of series of curves obtained on a multi-crystal triaxial X-ray diffractometer with high accuracy and speed [2].

## 2. Related works

The analysis of X-ray rocking curves is described in the work [1], where the dependence of the shape of the curves on the defects of the studied metal alloys is analyzed. It is shown that based on the parameters of the shape of the curves, in particular, the half-width (the width of the peak at half-height), it is possible to diagnose the mechanical and other properties of the studied materials. In the work [15], the defective structure of CdTe crystals is investigated by analyzing X-ray rocking curves. Such studies are important since the structural perfection of the crystals significantly affects the quality of the detectors made on their basis [16]. In the considered works [14-16], the experimental X-ray curves contained a certain level of noise, which limits the accuracy of their analysis.

Signal processing using bilateral filtering is described in the works [17-19]. The possibilities of bilateral filtering are considered in the work [17] using the example of medical image processing. As a result of such filtering, the signal-to-noise ratio on the studied images has been increased. However, bilateral filtering tools can be used to process not only images, but also one-dimensional X-ray curves. Bilateral filtering using the Fourier transform is described in the work [18]. The possibilities of bilateral filtering in image processing are also considered in the works [19, 20]. Analysis of the considered works [14, 17, 20] shows that bilateral filtering provides a reduction in the noise level with minor signal distortions. At the same time, there is a problem of choosing the parameters of the bilateral filter.

A promising direction of noise filtering on signals is the use of artificial neural networks (ANN). In the work [21], the possibilities of ANN in filtering noise on speech and biomedical signals are considered. Signal filtering is performed by various types of ANN, in particular, autoencoders [22], convolutional neural networks and recurrent neural networks [23]. Despite their effectiveness, ANN require special training before application. In addition, the output signals of ANN with a high probability may contain artifacts.

Thus, the analysis of the considered publications confirms the relevance of bilateral filtering and the need for software development for automatic bilateral filtering of X-ray curves.

## 3. Proposed mathematical model of bilateral filtering of X-ray curves

Digital X-ray curves  $I_h(\omega)$  describe the dependence of the intensity of the curve  $I_h$  on the rotation angle  $\omega$ , with the values of  $I_h$  and  $\omega$  given at  $Q$  points. Such curves are processed programmatically

as arrays  $I_h = I_h(i)$  and  $\omega = \omega(i)$ , where  $i = 0, \dots, Q-1$ ;  $I_h(i)$  is the intensity of the curve at point number  $i$ ;  $\omega(i)$  is the angular value of point number  $i$ .

Bilateral filtering [14] consists in convolution of the initial curve  $I_h$  with the filter kernel  $w_B$  of size  $M_w$  elements according to the formula

$$I_{hB}(i) = \sum_{m=0}^{M_w-1} I_h(i - m + m_c) \cdot w_B(m), \quad (1)$$

where  $I_{hB}$  is the curve after filtering (of the same size as  $I_h$ );  $M_w$  is the size of the filter kernel;  $m_c$  is the element number for the center of the filter kernel.

The operation of convolution of the signal  $I_h$  with the kernel  $w_B$  is simply written as

$$I_{hB} = I_h * w_B. \quad (2)$$

The kernel  $w_B$  of the bilateral filter is described by the formula

$$w_B(m) = \exp\left(\frac{-(m - m_c)^2}{2\sigma_{BS}^2}\right) \cdot \exp\left(\frac{-(I_h(m) - I_C)^2}{2\sigma_{BI}^2}\right), \quad (3)$$

where  $m = 0, \dots, M_w-1$ ;  $m$  is the kernel element number;  $M_w$  is the size of the filter kernel;  $\sigma_{BS}$  is the standard deviation (SD) of the bilateral filter kernel in the spatial (angular) domain;  $\sigma_{BI}$  is the standard deviation of the bilateral filter kernel in the intensity domain;  $m_c$  is the element number for the center of the filter kernel;  $I_h(m)$  is the intensity of the curve point corresponding to the kernel element with number  $m$ ;  $I_C$  is the intensity of the curve point corresponding to the center of the kernel.

Thus, the bilateral filter is a combination of two Gaussian filters: one filter performs processing in the spatial domain (with SD  $\sigma_{BS}$ ), and the other performs processing in the intensity domain (with SD  $\sigma_{BI}$ ). The bilateral noise filtering method allows to preserve the clarity of the curve peaks, since this method uses spatially weighted averaging of the curve intensity. That is, in the peak region, the smoothing will be less and the peak shape will be preserved, and in the region with a smooth change in brightness, the noise smoothing will be stronger.

The size  $M_w$  of the filter kernel  $w_B$  is calculated taking into account the  $3\sigma$  rule for a one-dimensional Gaussian distribution. Similarly, the SD  $\sigma_{BI}$  of the kernel in the intensity domain is calculated according to the  $3\sigma$  rule:

$$\sigma_{BI} = 3 \cdot \sigma_N, \quad (4)$$

where  $\sigma_N$  is the noise level on the X-ray curve.

Since on the experimental X-ray curves are dominated the Gaussian noise [15, 24], as the noise level  $\sigma_N$  its standard deviation is used.

The high-frequency component  $I_{hNC}$  is extracted by convolution of the initial curve  $I_h$  with the kernel of the high-frequency Laplace filter  $w_L$  [24], which is described by the formula:

$$w_L = (-1, 2, -1). \quad (5)$$

For the obtained high-frequency component  $I_{hNC}$ , its histogram  $h_N$  is constructed, defined by  $Q_h$  for intervals (bins) (Figure 1).

In order to simplify the analysis of the histogram and to reduce its random deviations, the convolution of the initial histogram  $h_N$  with the kernel of the Gaussian filter (with SD  $\sigma_{HG}$ ; for example,  $\sigma_{HG}=1$ ) is performed, as a result of which the smoothed histogram  $h_{NF}$  is calculated. In the resulting histogram, the central peak mainly corresponds to noise (minor deviations from the average value), and the other (peripheral) parts of the histogram correspond to the high-frequency component of the useful signal (significant deviations from the average value).

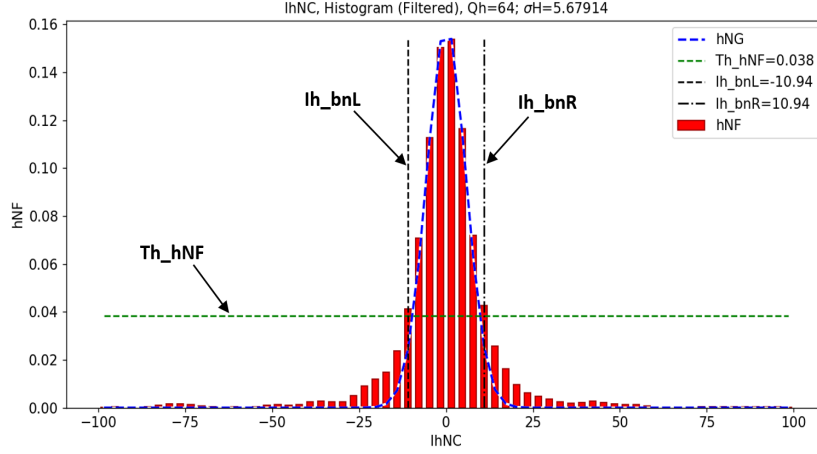


**Figure 1:** Smoothed histogram  $h_{NF}$  for the high-frequency component  $I_{hNC}$  of the signal and its main parameters.

The central peak of the histogram is extracted using the threshold  $Th_{hNF}$ ; the peak includes the histogram elements whose values exceed  $Th_{hNF}$ . The threshold  $Th_{hNF}$  value is calculated using the empirical formula:

$$Th_{hNF} = h_{NF\_max} \cdot kTh, \quad (6)$$

where  $h_{NF\_max}$  is the maximum value of the  $h_{NF}$  histogram;

$kTh$  is the threshold coefficient for extracting the histogram peak (for example,  $kTh = 0.25$ ).

The left boundary  $Ih_{nbL}$  of the histogram peak is defined as the smallest  $I_{hNC}$  value that exceeds the threshold  $Th_{hNF}$ . The right boundary  $Ih_{nbR}$  of the  $h_{NF}$  histogram peak is defined as the largest  $I_{hNC}$  value that exceeds the threshold  $Th_{hNF}$ . For the histogram peak (in the range from  $Ih_{nbL}$  to  $Ih_{nbR}$ ), its SD  $\sigma_{H0}$  is calculated.

Taking into account the convolution of the initial histogram  $h_N$  with the Gaussian filter kernel (with SD  $\sigma_{HG}$ ), the exact value of SD  $\sigma_H$  of the histogram peak is calculated by the formula:

$$\sigma_H = \sqrt{\sigma_{H0}^2 - \sigma_{HG}^2}. \quad (7)$$

After that, the Gaussian distribution  $h_{NG}$  (with SD  $\sigma_H$ ) is calculated, which describes the central peak of the histogram (Figure 1). The noise level  $\sigma_N$  is calculated based on such values of the high-frequency component  $I_{hNC}$  that correspond mainly to noise (and not to sharp changes in the useful signal) and are in the interval  $(ThIh_{min}, ThIh_{max})$ . The limits of the interval are calculated by empirical formulas:

$$ThIh_{min} = -\sigma_H \cdot k_\sigma, \quad (8)$$

$$ThIh_{max} = \sigma_H \cdot k_\sigma, \quad (9)$$

where  $k_\sigma = 2$ .

The value of the coefficient  $k_\sigma = 2$  is chosen from the condition that in the interval  $(ThIh_{min}, ThIh_{max})$  the values of the histogram  $h_{NF}$  are close to the normal distribution  $h_{NG}$  (since Gaussian noise on the X-ray curve is analyzed). With a narrower interval  $(ThIh_{min}, ThIh_{max})$ , part of the noise values will not be taken into account, and with a wider interval, the values of the useful signal in  $I_{hNC}$  will be taken into account.

The obtained value of the noise level  $\sigma_N$  is used to calculate the SD  $\sigma_{BI}$  of the bilateral filter kernel in the intensity domain according to formula (4).

The value SD  $\sigma_{BS}$  of the bilateral filter kernel in the spatial (angular) domain is determined based on the given value of the coefficient  $k_N$  of the noise level reduction as a result of filtering. The coefficient  $k_N = \sigma_{NC} / \sigma_N$  is calculated as the ratio of the noise SD  $\sigma_{NC}$  after filtering to the SD  $\sigma_N$  of

the noise before filtering. If the noise level on the signal  $I_h$  is equal to  $\sigma_N$ , then after smoothing the signal with the kernel  $w_G$  of the Gaussian filter with the SD  $\sigma_{BS}$ , the noise level  $\sigma_{NC}$  after filtering is equal to [24]:

$$\sigma_{NC} = \sigma_N \sqrt{\sum_{m=0}^{M_w-1} w_G^2(m)}, \quad (10)$$

where  $M_w = (2[3 \cdot \sigma_{BS}] + 1)$  is the number of elements of the filter kernel. From formula (10), the value of the coefficient  $k_N$  is equal to:

$$k_N = \sqrt{\sum_{m=0}^{M_w-1} w_G^2(m)}. \quad (11)$$

According to formula (11), for SD  $\sigma_{BS} = 3$  (the number of elements is used as the unit of measurement) there is the value  $k_N = 0.307094$ ; for  $\sigma_{BS} = 5$  there is the value  $k_N = 0.237978$ . The value of  $\sigma_{BS}$  is chosen so that the coefficient  $k_N$  does not exceed the threshold value (according to the filtering conditions of a certain type of signal).

#### 4. Software implementation of bilateral filtering

The software for bilateral filtering of X-ray curves is implemented in Python [25] based on the developed mathematical model (section 2). Bilateral filtering of X-ray curves  $I_h(\omega)$  involves the following stages:

1. Reading the initial curve  $I_h(\omega)$  from a text file.
2. Calculating the high-frequency component of the signal  $I_{hNC}$  by convolving the initial curve  $I_h$  with the Laplace filter kernel  $w_L$  (5).
3. Calculating the histogram  $h_N$  for the high-frequency component  $I_{hNC}$  using the «histogram» function of the numpy library.
4. Calculating the smoothed histogram  $h_{NF}$  by convolving the initial histogram  $h_N$  with the Gaussian filter kernel (with SD  $\sigma_{HG}$ ) using the «gaussian\_filter1d» function of the scipy library.
5. Selection of the central peak of the histogram based on the threshold  $Th\_hNF$  (6), calculation of its left  $Ih\_nbL$  and right  $Ih\_nbR$  boundaries, calculation of the SD  $\sigma_H$  of the histogram peak (7).
6. Calculation of the noise level  $\sigma_N$  based on the values of the high-frequency component  $I_{hNC}$ , which are in the permissible interval ( $ThIh\_min$ ,  $ThIh\_max$ ) (8, 9).
7. Calculation of the SD  $\sigma_{BI}$  of the kernel in the intensity domain through the SD of the noise  $\sigma_N$  according to the formula (4).
8. Determination of the SD  $\sigma_{BS}$  of the kernel in the spatial (angular) domain, provided that the permissible value of the noise level reduction coefficient  $k_N$  (11).
9. Calculation for each point of the X-ray curve (with number  $i$ ) of the bilateral filter kernel  $w_B$  (3), performing bilateral filtering by convolution of the intensities of the curve points  $I_h(\omega)$  and the kernel  $w_B$  according to the formula (1).
10. Visualization of the calculated curve  $I_{hB}(\omega)$  after bilateral filtering using the matplotlib library and saving the curve to a file.

Using the developed program, bilateral filtering of 20 X-ray curves of the training dataset is performed. During the processing of such curves, processing parameters are determined that provide the required reduction in the noise level (according to the value of the coefficient  $k_N$  from the formula (11)) while maintaining the clarity of the peaks. As a result, the following values of the program parameters are set:

- SD  $\sigma_{HG} = 1$  (SD of the Gaussian filter kernel, which is used to smooth the histogram  $h_N$ ).
- $kTh = 0.25$  (threshold coefficient for histogram peak extraction, which is determined by the minimum of the mean square difference between the histogram  $h_{NF}$  and the Gaussian distribution  $h_{NG}$  in the interval from  $Ih\_nbL$  to  $Ih\_nbR$ ).
- SD  $\sigma_{BS} = 5$  (SD  $\sigma_{BS}$  of the bilateral filter kernel in the spatial (angular) domain).

## 5. Results of bilateral filtering of X-ray curves by the developed software

### 5.1. Results of bilateral filtering of experimental X-ray curve # 1

Let us consider an example of bilateral filtering of experimental X-ray curve  $I_h(\omega)$  # 1 (Figure 2), which belongs to the training dataset of curves. The intensity of the curve is given in  $Q$  points. When visualizing such curves, it is especially effective to use a logarithmic scale for the intensity of the curve, since in this case not only peaks are well visualized, but also signal values for low intensities (the so-called 'tails' of the curves) (Figure 2a), which contain important information about the objects under study.

Next, based on the initial X-ray curve  $I_h(\omega)$ , the value of the high-frequency component  $I_{hNC}(\omega)$  is calculated (Figure 3). In order to improve the visualization of noise (to which small values of  $I_{hNC}$  correspond), the graph shows only the values of  $I_{hNC}$  that are within the permissible range (for example, from -100 to 100 in conventional units).

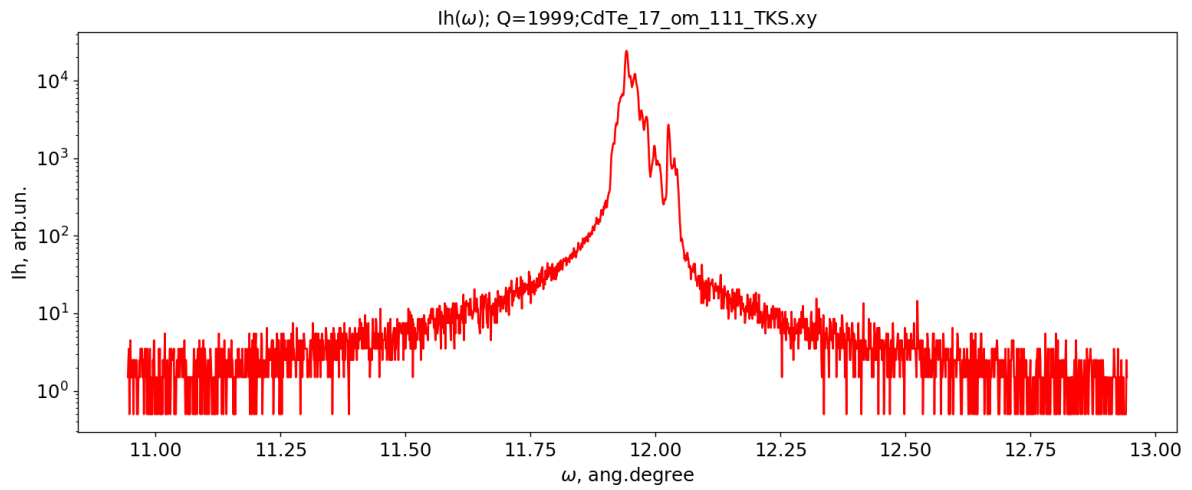
Based on the high-frequency component of the signal  $I_{hNC}$ , its histogram  $h_N$  is calculated, and by convolving the initial histogram  $h_N$  with the kernel of the Gaussian filter (with SD  $\sigma_{HG}$ ), a smoothed histogram  $h_{NF}$  is calculated (Figure 4).

Taking into account the threshold  $Th\_hNF$ , the left  $Ih\_nbL$  and right  $Ih\_nbR$  boundaries for the central peak of the histogram are calculated, and the SD  $\sigma_H$  of the histogram peak is also calculated. The resulting normal distribution  $h_{NG}$  (with SD  $\sigma_H$ ) quite accurately describes the peak of the histogram, which corresponds to Gaussian noise.

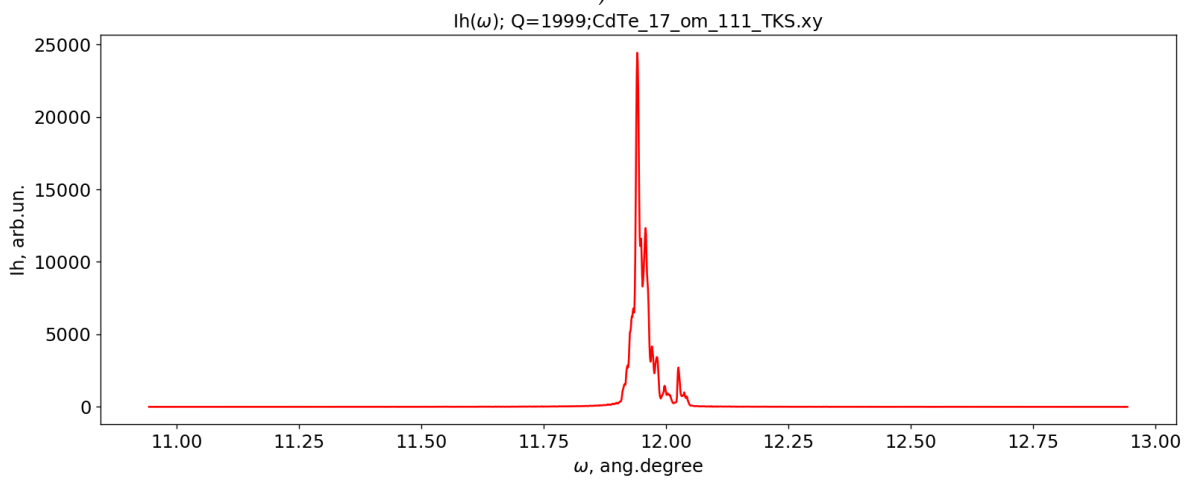
Taking into account the SD  $\sigma_H$  of the histogram peak, the values of the permissible interval ( $ThIh\_min$ ,  $ThIh\_max$ ) for the values of the high-frequency component  $I_{hNC}$  are calculated (Figure 5). The noise level  $\sigma_N$  is calculated based on the values of the high-frequency component  $I_{hNC}$ , which are in the permissible interval.

Taking into account the calculated noise SD  $\sigma_N$ , the SD  $\sigma_{BI}$  of the bilateral filter kernel in the intensity domain was calculated and value of the SD  $\sigma_{BS} = 5$  was determined for the kernel in the spatial (angular) domain. The SD  $\sigma_{BS}$  of the bilateral filter kernel is chosen so that the noise level in areas with a smooth change in intensity (without peaks) is reduced by  $k_N=0.24$  times. After this, bilateral filtering of the initial curve  $I_h(\omega)$  is performed. On the obtained curve  $I_{hB}(\omega)$  after bilateral filtering, a significant reduction in the noise level is observed while maintaining the clarity of all peaks (Figure 6). The reduction in the noise level on the  $I_{hB}(\omega)$  curve compared to the initial curve is particularly noticeable (Figure 7).

The filtered curve  $I_{hB}(\omega)$  contains mainly the useful signal, which simplifies and increases the accuracy of its subsequent analysis. For example, the angular intensity distribution is visually better perceived on the filtered curve  $I_{hB}(\omega)$  compared to the initial  $I_h(\omega)$ . Software processing of the curves  $I_{hB}(\omega)$  allows to accurately determine the coordinates of the peaks, their half-widths (width at half height), the slopes of the angular intensity distributions for local areas and other parameters that carry important diagnostic information about the structural perfection of the studied materials.



a)



b)

**Figure 2:** Initial X-ray curve  $I_h(\omega)$  # 1 obtained from a CdTe crystal and read from the file 'CdTe\_17\_om\_111\_TKS.xy' [24]: a) logarithmic scale by intensity; b) linear scale by intensity.

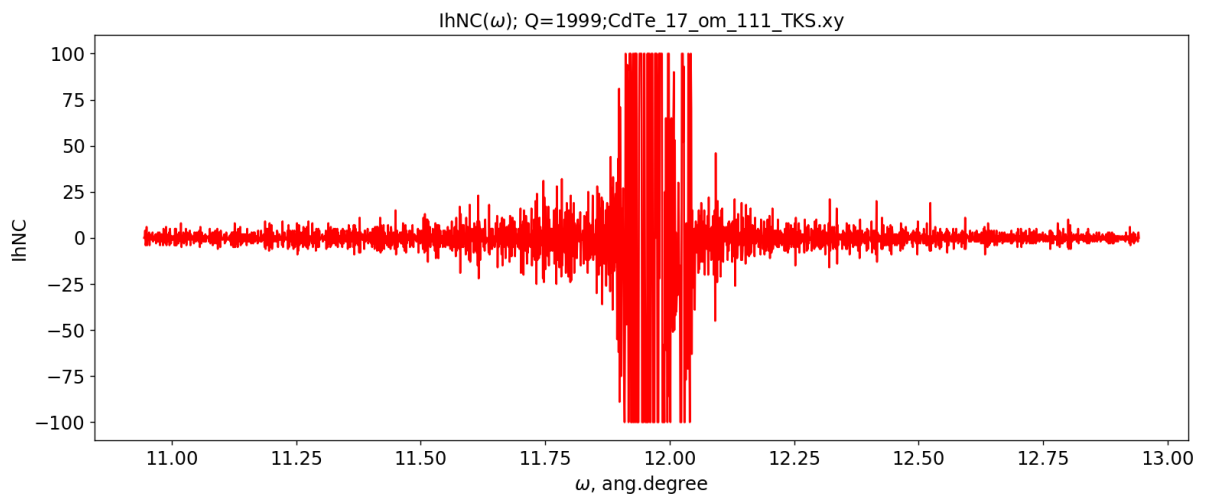


**Figure 3:** Values of the high-frequency component  $I_{hNC}(\omega)$  calculated for the initial X-ray curve  $I_h(\omega)$  (Figure 2).

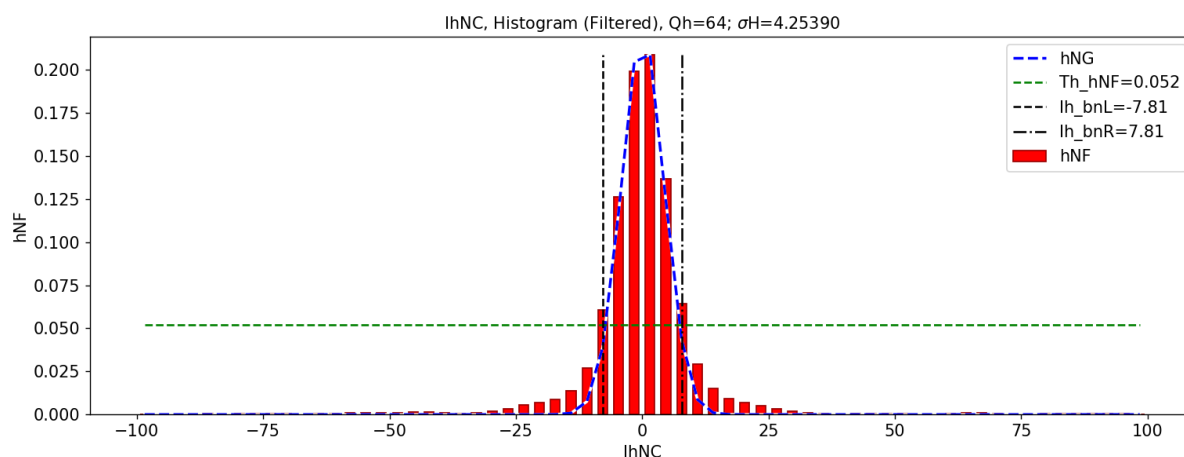


**Figure 4:** Smoothed histogram  $h_{NF}$  for the noise component  $I_{hNC}$  (Figure 3).

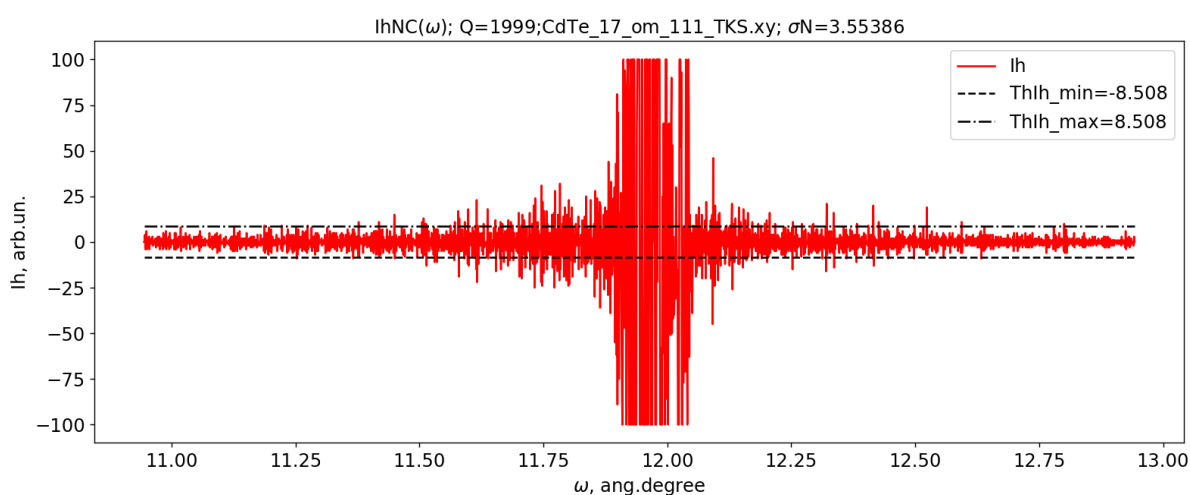


**Figure 5:** The value of the high-frequency component  $I_{hNC}(\omega)$  (Figure 3) with an permissible interval ( $Thlh_{min}$ ,  $Thlh_{max}$ ) for noise.

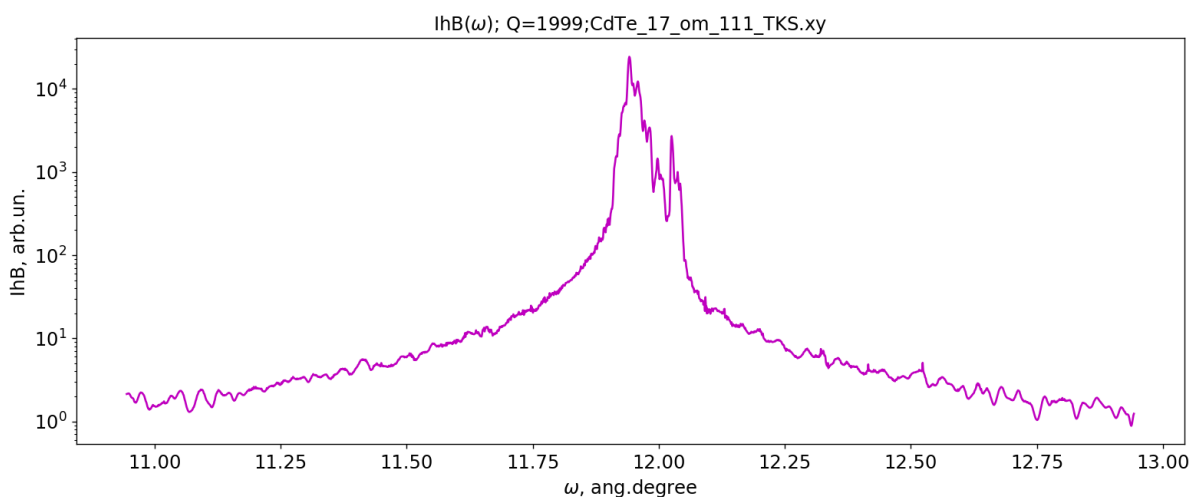


**Figure 6:** X-ray curve  $I_{hB}(\omega)$  after bilateral filtering which calculated on the basis of the initial curve  $I_h(\omega)$  (Fig. 2).

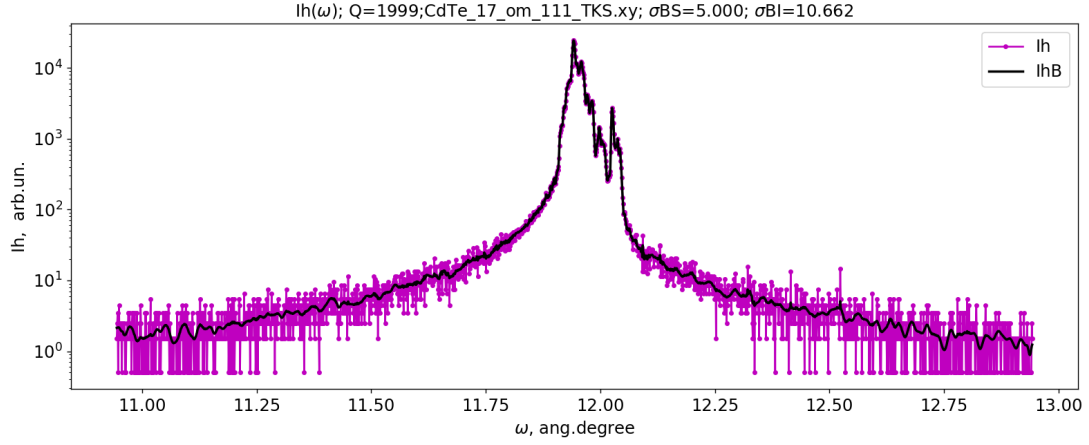


**Figure 7:** Initial X-ray curve  $I_h(\omega)$  (Figure 2) and X-ray curve  $I_{hB}(\omega)$  after bilateral filtering (Figure 6).

## 5.2. Results of bilateral filtering of experimental X-ray curve # 2

An example of bilateral filtering of the experimental X-ray curve  $I_h(\omega)$  # 2 (Figure 8), which belongs to the test dataset of curves, shall be considered. Based on the initial X-ray curve  $I_h(\omega)$ , the value of the high-frequency component  $I_{hNC}(\omega)$  and its histogram  $h_N$  are calculated. By convolving the initial histogram  $h_N$  with the Gaussian filter kernel (with SD  $\sigma_{HG}$ ), the smoothed histogram  $h_{NF}$  is calculated (Figure 9). The left  $I_{h\_nbL}$  and right  $I_{h\_nbR}$  boundaries for the central peak of the histogram are calculated, and the SD  $\sigma_H$  of the histogram peak is also calculated. The obtained normal distribution  $h_{NG}$  (with SD  $\sigma_H$ ) describes the peak of the histogram quite accurately, which confirms the correctness of the selected values of SD  $\sigma_{HG}$  and the threshold coefficient  $kTh$  (established based on the analysis of the X-ray curves of the training sample).

Using the SD  $\sigma_H$  of the histogram peak, the values of the permissible interval ( $ThIh\_min$ ,  $ThIh\_max$ ) for the values of the high-frequency component  $I_{hNC}$  are calculated (Figure 10). As can be seen in Figure 10, the  $I_{hNC}$  values in the left and right parts are limited by the interval ( $ThIh\_min$ ,  $ThIh\_max$ ). This means that the interval ( $ThIh\_min$ ,  $ThIh\_max$ ) correctly limits the noise value on the  $I_{hNC}$  graph, since it is in the left and right parts of the curve that the noise level is significant compared to the level of the useful signal. The noise level  $\sigma_N$  is calculated based on the  $I_{hNC}$  values that are in the permissible interval.

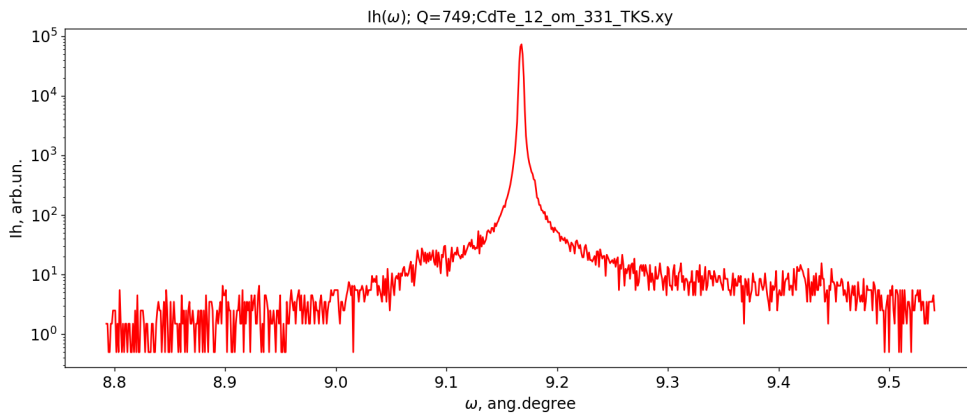


**Figure 8:** Initial X-ray curve  $I_h(\omega)$  # 2 which obtained from the CdTe crystal and read from the «CdTe\_12\_om\_331\_TKS.xy» file [24].

Based on the obtained noise SD  $\sigma_N$ , the SD  $\sigma_{BI}$  of the bilateral filter kernel in the intensity domain was calculated, and value of the SD  $\sigma_{BS} = 5$  was determined for the kernel in the spatial (angular) domain. Bilateral filtering of the initial curve  $I_h(\omega)$  is performed. On the obtained curve  $I_{hB}(\omega)$  after bilateral filtering, a significant smoothing of noise is observed while maintaining the clarity of the peaks, which is especially noticeable in comparison with the initial curve (Figure 11). The curve  $I_{hB}(\omega)$

after bilateral filtering contains mainly a useful signal, which allows for a more accurate analysis of its shape and the detection of patterns in the angular intensity distribution. In particular, on the filtered curve  $I_{hB}(\omega)$  a local maximum for the angle  $\omega = 9.42^\circ$  is clearly observed, which is barely noticeable on the initial curve. Accurate determination of angular coordinates for the peaks of X-ray curves allows, in particular, to determine with high accuracy lattice deformations and changes in interplanar distances for the crystals under study.

Bilateral filtering of 10 experimental X-ray curves of the test dataset is performed, and in all cases similar results are obtained: a significant reduction in their noise level while preserving the shape of the useful signal.

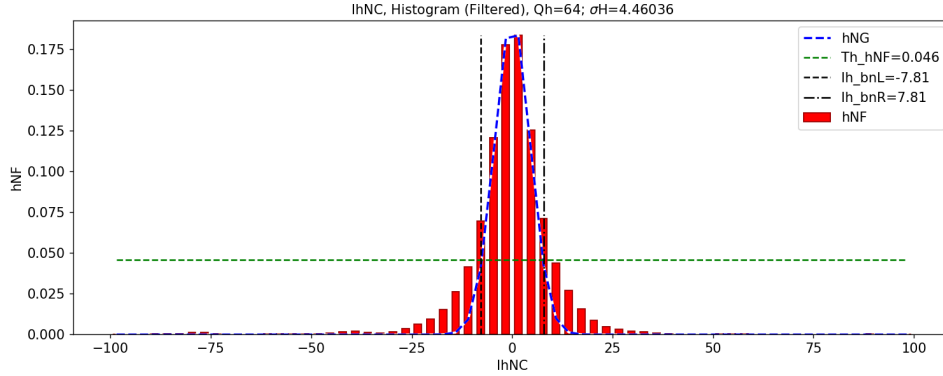


**Figure 9:** Smoothed histogram  $h_{NF}$  of the noise component  $I_{hNC}$  for the curve  $I_h(\omega)$  (Figure 8).

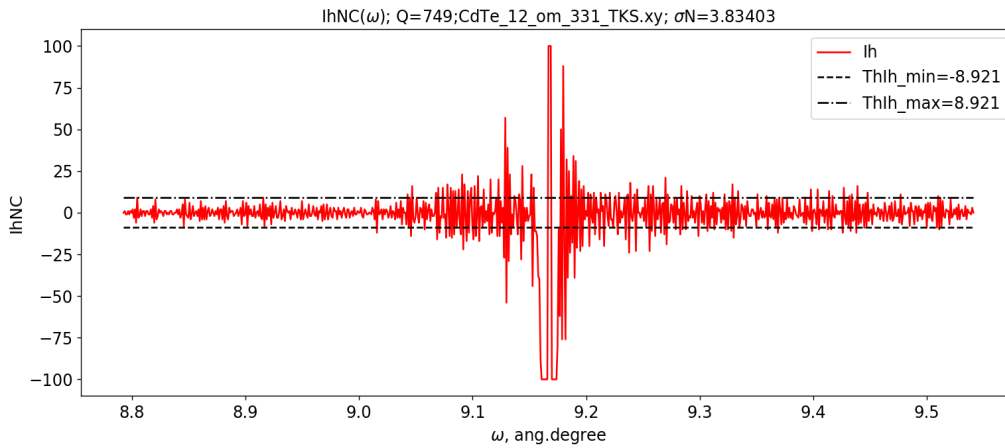


**Figure 10:** The value of the high-frequency component  $I_{hNC}(\omega)$  for the  $I_h(\omega)$  curve (Figure 8) with the permissible interval  $(ThIh_{min}, ThIh_{max})$  for noise.

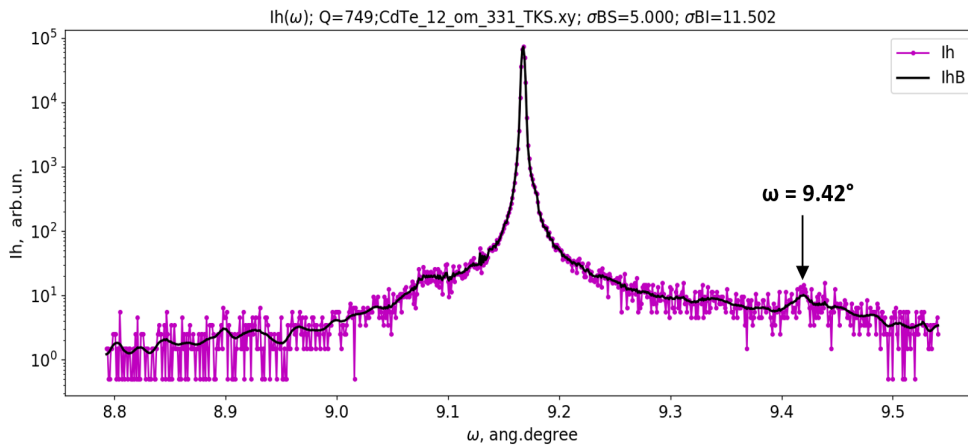


**Figure 11:** Initial X-ray curve  $I_h(\omega)$  (Figure 8) and X-ray curve  $I_{hB}(\omega)$  after bilateral filtering.

## 6. Conclusion

Software has been developed for noise removal on digital X-ray curves  $I_h(\omega)$  using a bilateral filter whose parameters are determined automatically. The digital bilateral filter has been constructed as a combination of two Gaussian filters that perform signal processing in the intensity domain and in the spatial (angular) domain. A mathematical model has been developed for calculating the noise level  $\sigma_N$  on the initial X-ray curve and the parameters of the bilateral filter. The following filter parameters were used: the standard deviation  $\sigma_{BI}$  of the filter kernel in the intensity domain and standard deviation  $\sigma_{BS}$  in the angular domain. The high-frequency component  $I_{hNC}$  of the X-ray curve has been extracted by a Laplace filter. The histogram  $h_{NF}$  of the high-frequency component has been calculated, and permissible interval ( $ThIh_{min}$ ,  $ThIh_{max}$ ) for noise values on the high-frequency component has been set. The noise level  $\sigma_N$  has been calculated based on the high-frequency component  $I_{hNC}$ , taking into account the established permissible interval.

The software for automatic bilateral filtering of X-ray curves has been developed in the Python language. The parameters of bilateral filtering have been set taking into account the results of processing 20 experimental X-ray curves of the training dataset. The value  $\sigma_{HG} = 1$  has been set for the SD of the Gaussian filter kernel, which is used to smooth the initial histogram. The value  $kTh = 0.25$  has been set for the threshold coefficient of the histogram peak selection. The SD  $\sigma_{BS}$  of the bilateral filter kernel has been chosen so that the noise level in areas with a smooth change in intensity (without peaks) is reduced by  $k_N = 0.24$  times.

Bilateral filtering of 10 experimental X-ray curves of the test dataset has been performed. It has been shown that bilateral filtering of X-ray curves allows not only to significantly reduce their noise level, but also to preserve the shape of the useful signal.

## Declaration on Generative AI

The author(s) have not employed any Generative AI tools.

## References

- [1] K.G.V. Siva Kumar, R. Oruganti, P. Chatterjee, X-Ray Rocking Curve Measurements of Dislocation Density and Creep Strain Evolution in Gamma Prime-Strengthened Ni-Base Superalloys, *Metall Mater. Trans. A* 50 (2019) 191–198. doi: 10.1007/s11661-018-4971-y.
- [2] SmartLab SE. Multipurpose X-ray Diffraction System with Built-In Intelligent Guidance, 2024. URL: <https://rigaku.com/products/x-ray-diffraction-and-scattering/xrd/smartlab-se>
- [3] S. Palani, *Principles of Digital Signal Processing*, Springer Cham., 2022.
- [4] L. Chyrun, V. Vysotska, S. Tchynetskyi, Y. Ushenko, D. Uhryn, Information Technology for Sound Analysis and Recognition in the Metropolis based on Machine Learning Methods, *International Journal of Intelligent Systems and Applications (IJISA)* 16 (6) (2024) 40-72. doi: 10.5815/ijisa.2024.06.03.
- [5] R.A. Abtan, Image Enhancement using Adaptive Median Filter, *International Journal of Scientific Research in Science, Engineering and Technology (IJSRSET)* 10 (4) (2023) 236-243. doi: 10.32628/IJSRSET23102118.
- [6] P.G. Malghan, M.K. Hota, 50Hz Power Line Interference Removal from an Electrocardiogram Signal Using a VME-DWT-Based Frequency Extraction and Filtering Approach, *International Journal of Image, Graphics and Signal Processing (IJIGSP)* 16 (4) (2024) 56-73. doi: 10.5815/ijigsp.2024.04.05.
- [7] A.K. Bansal, A Study on the Fast Fourier Transform Applications, *Asian Journal of Basic Science & Research* 5 (2) 2023 29-39. doi: 10.38177/AJBSR.2023.5203.
- [8] B. Tang, Y. Ding, Y. Peng, J. Cao, Target localization algorithm based on improved short-time Fourier transform, *Digital Signal Processing* 155 (2024) 104734. doi: 10.1016/j.dsp.2024.104734.
- [9] E. Rajaby, S.M. Sayedi, A structured review of sparse fast Fourier transform algorithms, *Digital Signal Processing* 123 (2022) 103403. doi: 10.1016/j.dsp.2022.103403.

- [10] J. Isabona, A.L. Imoize, S. Ojo, Image Denoising based on Enhanced Wavelet Global Thresholding Using Intelligent Signal Processing Algorithm, *International Journal of Image, Graphics and Signal Processing (IJIGSP)* 15 (5) (2023) 1-16. doi: 10.5815/ijigsp.2023.05.01.
- [11] S.E. Olukanni, J. Isabona, I. Odesanya, Enhancing Lte Rss for a Robust Path Loss Analysis with Noise Removal, *International Journal of Image, Graphics and Signal Processing (IJIGSP)* 15 (3) (2023) 60-68. doi: 10.5815/ijigsp.2023.03.05.
- [12] Y. Zhang, Adaptive block level bilateral filtering algorithm, *Applied and Computational Engineering* 17 (2023) 77-85. doi: 10.54254/2755-2721/17/20230917.
- [13] F. Spagnolo, P. Corsonello, F. Frustaci, S. Perrim, Approximate bilateral filters for real-time and low-energy imaging applications on FPGAs, *The Journal of Supercomputing* 80 (2024) 15894–15916. doi: 10.1007/s11227-024-06084-y.
- [14] S. Balovsyak, M. Borchha, M. Gregus ml., Kh. Odaiska, N. Serpak, Automatic Processing of Digital X-ray Medical Images by Bilateral Filtration Method, in: *Proceedings of the 2nd International Workshop on Intelligent Information Technologies and Systems of Information Security (IntellTSIS 2021)*, March 24-26, 2021, ceur-ws.org, Khmelnytskyi, Ukraine, 2021, pp. 280-294.
- [15] I.M. Fodchuk, A.R. Kuzmin, I.I. Hutsuliak, M.D. Borchha, V.O. Kotsyubynsky, Defect structure of high-resistance CdTe:Cl single crystals and MoOx/CdTe:Cl/MoOx heterostructures according to the data of high-resolution X-ray diffractometry, *Semiconductor Physics, Quantum Electronics and Optoelectronics* 26(4) (2023) 415-423. doi: 10.15407/spqeo26.04.415.
- [16] G. Yang, G. Park, Deformation of single crystals, polycrystalline materials, and thin films: A review, *Materials* 12 (12) (2019). doi: 10.3390/ma12122003.
- [17] V. Anoop, P. R. Bipin, Medical Image Enhancement by a Bilateral Filter Using Optimization Technique, *Journal of Medical Systems* 43/ 240 (2019) 1-12. doi: 10.1007/s10916-019-1370-x.
- [18] Y. Sumiya, N. Fukushima, K. Sugimoto, S.-i. Kamata, Extending Compressive Bilateral Filtering For Arbitrary Range Kernel, in: *IEEE International Conference on Image Processing (ICIP)*, Abu Dhabi, United Arab Emirates, 2020, pp. 1018-1022, doi: 10.1109/ICIP40778.2020.9191123.
- [19] X.-Y. Jia, C.-L. DongYe, Seismic section image detail enhancement method based on bilateral texture filtering and adaptive enhancement of texture details, *Nonlin. Processes Geophys.* 27 (2020) 253–260. doi: 10.5194/npg-27-253-2020.
- [20] G. Liu, The Novel Bilateral Quadratic Interpolation Image Super-resolution Algorithm, *International Journal of Image, Graphics and Signal Processing (IJIGSP)* 13 (3) (2021) 55-61. doi: 10.5815/ijigsp.2021.03.05.
- [21] H. Ferdous, S. Jahan, F. Tabassum, Md.I. Islam, The Performance Analysis of Digital Filters and ANN in De-noising of Speech and Biomedical Signal, *International Journal of Image, Graphics and Signal Processing (IJIGSP)* 15 (1) (2023) 63-78. doi: 10.5815/ijigsp.2023.01.06.
- [22] F. Franco. Signal Noise Removal Autoencoder with Keras, 2024. URL: <https://medium.com/codex/signal-noise-removal-autoencoder-with-keras-3dda589f8b24>.
- [23] T. Hovorushchenko, V. Alekseiko, V. Shvaiko, J. Ilchyshyna, A. Kuzmin, Information system for earth's surface temperature forecasting using machine learning technologies, *Computer Systems and Information Technologies* 4 (2024) 51–58. doi: 10.31891/csit-2024-4-7.
- [24] S.V. Balovsyak, Kh. S. Odaiska, Automatic Determination of the Gaussian Noise Level on Digital Images by High-Pass Filtering for Regions of Interest, *Cybernetics and Systems Analysis* 54 (4) (2018) 662-670. doi: 10.1007/s10559-018-0067-3.
- [25] G. Guillen, Digital Image Processing with Python and OpenCV, in: *Sensor Projects with Raspberry Pi. Maker Innovations Series*, Apress, Berkeley, CA, 2024, pp.105–147. doi: 10.1007/979-8-8688-0464-9\_5.